Rev. Roum. Sci. Techn.– Électrotechn. et Énerg.
Vol. **68**, *2*, pp. 176–181, Bucarest, 2023

INPUT-OUTPUT LINEARIZATION CONTROL BASED ON THE SLIDING MODE OF THE SQUIRREL CAGE MOTOR

KHEIRA MENDAZ[1], MOHAMED FLITTI[2]

Keywords: Squirrel cage motor; Sliding mode; Input-input linearization; Performance; Robustness.

Speed squirrel cage motor control is an area of research that has been in evidence for some time. In this paper, a nonlinear controller is presented for the squirrel cage motor drives, based on a combination between input-output feedback linearization control (IOLC) technique and sliding mode control (SMC) to create a new control which is sliding input-output linearization (SIOLC) control of squirrel cage motors, where the sliding mode control is used for controlling the speed of squirrel cage motor and the input-output linearization control applied for two input witch are flux and current. To test the robustness and performance of sliding input-output linearization control (SIOLC) we created a variety of internal and external parameters of the motor. The simulation results are done using Matlab/Simulink, which shows the robustness of the sliding input-output linearization control of squirrel cage motor responses.

1. INTRODUCTION

Squirrel cage motor is one of most machines used in variable speed applications because it has certain advantages, such as ease of manufacture and maintenance. It is also appreciated for its reliability and robustness. However, the simplicity of its mechanical structure is accompanied by a high complexity in the mathematical model (multi-variable and non-linear).

Due to the significant influence of nonlinearities on squirrel cage motor system dynamics, linear control techniques are quite good, and they may not meet the system specifications, mainly in the case of variable speed applications. Among the nonlinear techniques that ensure high performance and global decoupling between the outputs to control whatever the path profile imposed for the machine, one can mention the input-output linearization technique, and the other is the sliding mode technique [3, 5, 8].

The input-output linearization control is an analytical design approach that aims to reduce the original nonlinear problem to a simpler linear control problem. The nonlinear control system is designed using a two-step procedure [3, 4].

Firstly, a nonlinear process model synthesizes a nonlinear state feedback controller that linearizes the map between a newly manipulated input and the controlled output. In the second step, a linear pole placement controller is designed for the feedback linearized system.

The basic principle of sliding mode control consists of moving the system's state trajectory toward a predetermined sliding or switching surface and maintaining it around this latter with an appropriate switching logic. The design of a sliding mode controller has two steps: the definition of the adequate switching surface and the development of the control law (equivalent command and discontinuous command). The sliding mode control can offer good properties, such as insensitivity to parameter variations [9–11].

This article discusses a combination of two nonlinear controls: input-output linearization control and sliding mode control of squirrel cage motors.

2. MATHEMATICAL MODEL OF SQUIRREL CAGE MOTOR

The dynamic model of the squirrel cage motor is given below (dq rotating) wish rewritten in rotation reference frame [13]:

$$\frac{\mathrm{d}\Omega}{\mathrm{d}t} = \frac{T_\mathrm{e}}{J} - \frac{1}{J}T_\mathrm{l} - \frac{1}{J}f\Omega, \tag{1}$$

$$\frac{\mathrm{d}I_\mathrm{sd}}{\mathrm{d}t} = -\lambda\, I_\mathrm{sd} + w_\mathrm{s} I_\mathrm{sq} + \frac{K}{\tau_\mathrm{r}}\varphi_\mathrm{rq} + w_\mathrm{r}\, K\varphi_\mathrm{rd} + \frac{1}{\sigma L_\mathrm{s}}V_\mathrm{sd}, \tag{2}$$

$$\frac{\mathrm{d}I_\mathrm{sq}}{\mathrm{d}t} = -w_\mathrm{s} I_\mathrm{sd} - \lambda\, I_\mathrm{sq} - w_\mathrm{r}\, K\varphi_\mathrm{rd} - \frac{K}{\tau_\mathrm{r}}\varphi_\mathrm{rq} + \frac{1}{\sigma L_\mathrm{s}}V_\mathrm{sq}, \tag{3}$$

$$\frac{\mathrm{d}\varphi_{rd}}{\mathrm{d}t} = \frac{L_m}{\tau_r} I_{sd} - \frac{1}{\tau_r}\varphi_{rd} + (w_s - w_r)\varphi_\mathrm{rq}, \tag{4}$$

$$\frac{\mathrm{D}\varphi_{rq}}{\mathrm{d}t} = \frac{L_m}{\tau_r} I_{sq} - (w_s - w_r)\varphi_{rd} - \frac{1}{\tau_r}\varphi_{rq}, \tag{5}$$

with: $\tau_r = \frac{L_r}{R_r}$, $\sigma = 1 - \frac{L_m^2}{L_s\, L_r}$, $T_e = \frac{\mathrm{p}\,\mathrm{L_m}}{\mathrm{JL_r}}\left(\varphi_\mathrm{rd}\mathrm{I_{sq}} - \varphi_\mathrm{rq}\mathrm{I_{sd}}\right)$,

σ: scattering Blondel coefficient.

3. INPUT-OUTPUT LINEARIZATION CONTROL

The choice of outputs is according to the objectives of control. The current is chosen as the first output, while the second output is the square of the rotor flux to track the purposed control trajectory [3, 4].

$$y(\mathrm{x}) = \begin{bmatrix} h_1(x) \\ h_2(x) \end{bmatrix} = \begin{bmatrix} I_\mathrm{sq} \\ \varphi_\mathrm{dr}^2 + \varphi_\mathrm{qr}^2 \end{bmatrix}. \tag{6}$$

The time derivative of the system output $h_1(x)$ can be expressed as:

$$y_1 = h_1(x) = I_\mathrm{sq}, \tag{7}$$

$$\frac{\mathrm{d}y_1}{\mathrm{d}t} = \frac{\mathrm{d}h_1(x)}{\mathrm{d}t} = \frac{\mathrm{d}I_{sq}}{\mathrm{d}t}, \tag{8}$$

$$\frac{dy_1}{dt} = L_f h_1(x) + L_{gl}\, h_1(x)\; V_{sd} + L_{g2}\; h_1(x)\; V_{sq}, \tag{9}$$

$$\frac{\mathrm{d}y_1}{\mathrm{d}t} = -w_s I_{sd} - \lambda\, I_{sq} - w_r\, K\varphi_\mathrm{rd} - \frac{K}{\tau_r}\varphi_{rq} + \frac{1}{\sigma L_s}V_{sq}. \tag{10}$$

The degree of $h_1(x)$ is $r_1 = 1$.The time derivative of the system output $h_2(x)$ can be expressed as:

$$y_2 = h_2(x) = \varphi_\mathrm{r}^2 \tag{11}$$

$$\frac{\mathrm{d}y_2}{\mathrm{d}t} = \frac{\mathrm{d}h_2(x)}{\mathrm{d}t} = \frac{\mathrm{d}\varphi_\mathrm{r}^2}{\mathrm{d}t}, \tag{12}$$

$$\frac{\mathrm{d}y_2}{\mathrm{d}t} = L_\mathrm{f} h_2(x) + L_\mathrm{g1}\, h_2(x)\; V_\mathrm{sd} + L_\mathrm{g2}\; h_2(x)\; V_\mathrm{sq} \tag{13}$$

[1] Electrical engineering department, Faculty of sciences and technologies, University of Ain Temouchent, IRECOM laboratory Djillali Liabes unversity Sidi bel abbes, Algeria, kheira.mendaz@univ-temouchent.edu.dz
[2] Electrical engineering department, Faculty of sciences and technologies, University of Ain Temouchent, ICEPS laboratory Djillali Liabes unversity Sidi bel abbes, Algeria, mohammed.flitti@univ-temouchent.edu.dz

$$\varphi_r^2 = \varphi_{rd}^2 + \varphi_{rq}^2 \quad (14)$$

$$\frac{dy_2}{dt} = \frac{d\varphi_r^2}{dt} = \frac{2}{\tau_r}\left(L_m\left(\varphi_{dr}I_{sq} + \varphi_{qr}I_{sd}\right) - \left(\varphi_{rd}^2 + \varphi_{rq}^2\right)\right). \quad (15)$$

Note that for a controllable system, the total relative degree is defined as the sum of all the relative degrees; it must be less than or equal to the system order, $r \le n$, with n as the system order, and r is total relative degree [6, 7].

In the case of the squirrel cage motor system, it is easy to verify that the control can't appear for the first time in the first derivative of the outputs y_2, so we derivative the outputs $\frac{dy_2}{dt}$ for the second time as presented in the following [6]:

$$\frac{d^2y_2}{dt^2} = \frac{d^2h_2(x)}{dt^2} = \frac{d^2\varphi_r^2}{dt^2}, \quad (16)$$

$$\frac{d^2y_2}{dt^2} = L_f^2\, h_2(x) + L_{g1}\, L_f h_2(x)\; V_{sd} + L_{g2}\; L_f\, h_2(x)\; V_{sq} \quad (17)$$

$$\frac{d^2y_2}{dt^2} = \left(2\left(\frac{1}{\tau_r}\right)^2(2 + kL_m)\right)\left(\varphi_{rd}^2 + \varphi_{rq}^2\right) + \left(\frac{2\, n_p L_m}{\tau_r}\right)\left(\Omega\left(\varphi_{rd}I_{sq} + \varphi_{dr}I_{sq}\right)\right) - \left(\left(6\left(\frac{1}{\tau_r}\right)^2 L_m\right) + \left(\frac{2\,\lambda\, L_m}{\tau_r}\right)\right) + \left(2\left(\frac{L_m}{\tau_r}\right)^2\right)\left(I_{sd}{}^2 + I_{sq}{}^2\right) + \frac{2\, pL_m{}^2}{JL_r\sigma\, LS}\varphi_{dr}V_{sd} + + \frac{2\, p\, L_m{}^2}{JL_r\sigma\, LS}\varphi_{rq}V_{sq}. \quad (18)$$

The degree of $h_2(x)$ is $r_2 = 2$. The global relative degree is lower than the order n of the system $r = r_1 + r_2 = 3 < n < 5$.

The matrix defines a relation between the input (V_{sd}, V_{sq}) and the output (y_1, y_2) is given by the expression:

$$\begin{bmatrix} \frac{dy_1}{dt} \\ \frac{d^2y_2}{dt^2} \end{bmatrix} = A(x) + D(x)\begin{bmatrix} V_{ds} \\ V_{qs} \end{bmatrix}, \quad (19)$$

$$A(x) = \begin{bmatrix} L_f h_1(x) \\ L_f^2\, h_2(x) \end{bmatrix}, \quad (20)$$

$$L_f h_1(x) = -w_s I_{sd} - \lambda\, I_{sq} - w_r\, K\varphi_{rd} - \frac{K}{\tau_r}\varphi_{rq}. \quad (21)$$

$$L_f^2\, h_2(x) = \left(2\left(\frac{1}{\tau_r}\right)^2(2 + kL_m)\right)\left(\varphi_{rd}^2 + \varphi_{rq}^2\right) + \left(\frac{2\, pL_m}{\tau_r}\right)\left(\Omega\left(\varphi_{rd}I_{sq} + \varphi_{dr}I_{sq}\right)\right) - \left(\left(6\left(\frac{1}{\tau_r}\right)^2 L_m\right) + \left(\frac{2\,\lambda\, L_m}{\tau_r}\right)\right)\left(\varphi_{rq}I_{sq} + \varphi_{dr}I_{sd}\right) + \left(2\left(\frac{L_m}{\tau_r}\right)^2\right)\left(I_{sd}{}^2 + I_{sq}{}^2\right) \quad (22)$$

$$D(x) = \begin{bmatrix} L_{g1}\, L_f h_1 & L_{g2}\, L_f h_1 \\ L_{g1}\, L_f h_2 & L_{g2}\, L_f h_2 \end{bmatrix} = \begin{bmatrix} 0 & \frac{1}{\sigma L_s} \\ \frac{2\, pL_m{}^2}{JL_r\sigma\, LS}\varphi_{dr} & \frac{2\, pL_m{}^2}{JL_r\sigma\, LS}\varphi_{rq} \end{bmatrix} \quad (23)$$

The nonlinear feedback provides to the system a linear input/output relation:

$$\begin{bmatrix} \frac{dy_1}{dt} \\ \frac{d^2y_2}{dt^2} \end{bmatrix} = \begin{bmatrix} v_1 \\ v_2 \end{bmatrix}, \quad (24)$$

$$\begin{bmatrix} V_{ds} \\ V_{qs} \end{bmatrix} = D^{-1}(x)\begin{bmatrix} v_1 - L_f h_1(x) \\ v_2 - L_f^2\, h_2(x) \end{bmatrix}. \quad (25)$$

4. CURRENT AND FLUX LINEAR CONTROL

The internal inputs (V_1, V_2) are defined: [5, 6]

$$V_1 = \frac{dh_1(x)}{dt} = \frac{dI_{sq}}{dt} \quad (26)$$

$$V_2 = \frac{d^2y_2}{dt^2} = \frac{d^2\varphi_r^2}{dt^2} \quad (27)$$

$$V_1 = \frac{de_1}{dt} + K_{11}\, e_1 \quad (28)$$

$$V_2 = \frac{d^2e_2}{dt^2} + K_{21}\frac{de_2}{dt} + K_{22}\, e_2 \quad (29)$$

$$V_1 = \left(\frac{dI_{sqref}}{dt} - \frac{dI_{sq}}{dt}\right) + K_{11}\left(I_{sqref} - I_{sq}\right). \quad (30)$$

$$V_2 = \left(\frac{d^2\varphi_{rref}^2}{dt^2} - \frac{d\varphi_r^2}{dt}\right) + K_{21}\left(\frac{d\varphi_{rref}^2}{dt} - \frac{d\varphi_r^2}{dt}\right) + + K_{22}\left(\varphi_{rref}^2 - \varphi_r^2\right). \quad (31)$$

The error of the track is given by flowing equation:

$$\frac{de_1}{dt} K_{11}\, e_1 = 0, \quad (32)$$

$$\frac{d^2e_2}{dt^2} K_{21}\frac{de_2}{dt} + K_{22}\, e_2 = 0, \quad (33)$$

$$e_1 = I_{sqref} - I_{sq}, \quad (34)$$

$$\frac{de_1}{dt} = \frac{dI_{sqref}}{dt} - \frac{dI_{sq}}{dt}, \quad (35)$$

$$e_2 = \varphi_{rref}^2 - \varphi_r^{2,} \quad (36)$$

$$\frac{de_2}{dt} = \frac{d\varphi_{rref}^2}{dt} - \frac{d\varphi_r^2}{dt}, \quad (37)$$

$$\begin{bmatrix} V_{ds} \\ V_{qs} \end{bmatrix} = D^{-1}(x)\begin{bmatrix} v_1 - L_f h_1(x) \\ v_2 - L_f^2\, h_2(x) \end{bmatrix} = \begin{bmatrix} \left(\frac{dI_{sqref}}{dt} - \frac{dI_{sq}}{dt}\right) + K_{11}\left(I_{sqref} - I_{sq}\right) - L_f h_1(x) \\ \frac{d^2\varphi_{rref}^2}{dt^2} + K_{21}\left(\frac{d\varphi_{rref}^2}{dt} - \frac{d\varphi_r^2}{dt}\right) K_{22}\left(\varphi_{rref}^2 - \varphi_r^2\right) - L_f^2\, h_2(x) \end{bmatrix}, \quad (38)$$

where the coefficients K_{11}, K_{21}, K_{22} are chosen to satisfy asymptotic stability and excellent tracking [1]

$$\left(\frac{dI_{sqref}}{dt} - \frac{dI_{sq}}{dt}\right) + K_{11}\left(I_{sqref} - I_{sq}\right) = 0, \quad (39)$$

$$\left(\frac{d^2\varphi_{rref}^2}{dt^2} - \frac{d\varphi_r^2}{dt}\right) + K_{21}\left(\frac{d\varphi_{rref}^2}{dt} + \frac{d\varphi_r^2}{dt}\right) + K_{22}\left(\varphi_{rref}^2 - \varphi_r^2\right) \quad (40)$$

where: $\frac{dI_{sqref}}{dt} = 0$, $\frac{d^2\varphi_{rref}^2}{dt^2} = 0$, $\frac{d\varphi_{rref}^2}{dt} = 0$,

$$\frac{dI_{sq}}{dt} + K_{11}\, I_{sq} = K_{11}\, I_{sqref}, \quad (41)$$

$$\frac{d^2\varphi_r^2}{dt^2} + K_{21}\frac{d\varphi_r^2}{dt} + K_{22}\,\varphi_r^2 = K_{22}\,\varphi_{rref}^2. \quad (42)$$

From (41) and (42) the current and flux transfer function is given by the following equation:

$$\frac{I_{sq}}{I_{sqref}} = \frac{1}{1 + \frac{1}{K_{11}}p} = \frac{K}{1 + T\, p}. \quad (43)$$

$$\frac{\varphi_r^2}{\varphi_{rref}^2} = \frac{K_{22}}{K_{22} + K_{21}\, p + p^2} = \frac{\omega_n}{\omega_n{}^2 + 2\varepsilon\omega_n\, p + p^2}. \quad (44)$$

In closed loops, the current transfer functions have first-order dynamics, and flux transfer functions have second-order dynamics. By identifying them to the canonical form:

$$T = \frac{1}{K_{11}} \Rightarrow K_{11} = \frac{1}{T} = \frac{3}{T_r}, \quad (45)$$

with $T_r = 3\, T(\pm 5\%$, T_r is the response time, T is the time constant

$$\begin{cases} K_{21} = 2\varepsilon\omega_n \\ K_{22} = \omega_n{}^2 \end{cases}. \quad (46)$$

4.1 SPEED SLIDING MODE CONTROL

The motor speed Ω should track a specific reference speed

Ω_{ref} in the presence of load torque [9–11]. The system is controlled so that the error $e(t) = \Omega_{ref} - \Omega$ and its rate of change always moves towards a sliding surface. We take n = 1, the speed control manifold equations can be obtained as [11,12]:

$$S(\Omega) = \Omega_{ref} - \Omega \quad (47)$$

$$\frac{dS(\Omega)}{dt} = \frac{d\Omega_{ref}}{dt} - \frac{d\Omega}{dt} \quad (48)$$

$$T_e = \frac{p\ L_m}{J\ L_r}\ \varphi_{rd}\ I_{sq} \quad (49)$$

$$\frac{d\Omega}{dt} = \frac{T_e}{J} - \frac{1}{J}\ T_l - \frac{1}{J}\ f\Omega. \quad (50)$$

Substituting the expression of T_e defined by (49) in (50), we obtain:

$$\frac{d\Omega}{dt} = \frac{p\ L_m}{J\ L_r}\left(\varphi_{rd} I_{sq}\right) - \frac{1}{J}\ T_l - \frac{1}{J}\ f\Omega. \quad (51)$$

Substituting the expression of $\frac{d\Omega}{dt}$ defined by (51) in (48), we obtain:

$$\frac{dS(\Omega)}{dt} = \frac{d\Omega_{ref}}{dt} - \frac{p\ L_m}{J\ L_r}\left(\varphi_{rd} I_{sq}\right) - \frac{1}{J}\ T_l - \frac{1}{J}\ f\Omega. \quad (52)$$

Substituting the expression of I_{sq} by $I_{sq} = I_{sq}^{eq} + I_{sq}^{n}$ the command appears in the equation (53):

$$\frac{dS(\Omega)}{dt} = \frac{d\Omega_{ref}}{dt} - \frac{p\ L_m}{J\ L_r}\varphi_{rd}\left(I_{sq}^{eq} + I_{sq}^{n}\right) + \frac{1}{J}T_l + \frac{1}{J}\ f\Omega\ . \quad (53)$$

During the sliding mode and in the permanent regime,

$$S(\Omega) = 0, \frac{dS(\Omega)}{dt} = 0, I_{sq}^{n} = 0, \quad (54)$$

where the equivalent control is

$$I_{sq}^{eq} = \left(\frac{d\Omega_{ref}}{dt} + \frac{1}{J}T_l + \frac{1}{J}f\Omega\right)\frac{JL_r}{n_p L_m}\frac{1}{\varphi_{rd}}. \quad (55)$$

Consider the Lyapunov function [15]

$$V = \frac{1}{2}\ S(\Omega)^2. \quad (56)$$

From the Lyunov theorem know that if $\frac{dv}{dt}$ is negative definite, the system trajectory will be driven and attracted toward the sliding surface and remain sliding on it until the origin is reached asymptotically [14].

$$\frac{dv}{dt} = S(\Omega)\frac{dS(\Omega)}{dt} < 0. \quad (57)$$

During the convergence mode, the condition must be verified. We obtain:

$$\frac{dS(\Omega)}{dt} = -\frac{p\ L_m}{J\ L_r}\varphi_{rd}. \quad (58)$$

The following equation gives the correction factor (discontinuous command):

$$I_{sq}^{n} = K_{q1}\mathrm{sat}(S(\Omega)) \quad (59)$$

where:

$$\mathrm{sat}\left(S(\Omega)\right) = \begin{cases} S(\Omega) & \text{if } |S(\Omega)| < 0 \\ \frac{1}{\delta}S(\Omega) & \text{if } |S(\Omega)| > 0 \end{cases} \quad (60)$$

Figure 1 shows a combination between the sliding speed control and input-output linearization control (IOLC) of the squirrel cage motor that gives a new controller named sliding input-output linearization control (SIOLC). The output of the sliding speed controller delivers a reference current which will be an input for the internal input V_1 of the input-output linearization control of squirrel cage motors. The structure of the input-output linearization controller (IOLC) of the motor is composed of different controls; the first one is the nonlinear functions $A(x)$ and $D(x)$ which are drawn by using Lie derivatives. The second controls are the internal input. The final command is the decoupling matrix.

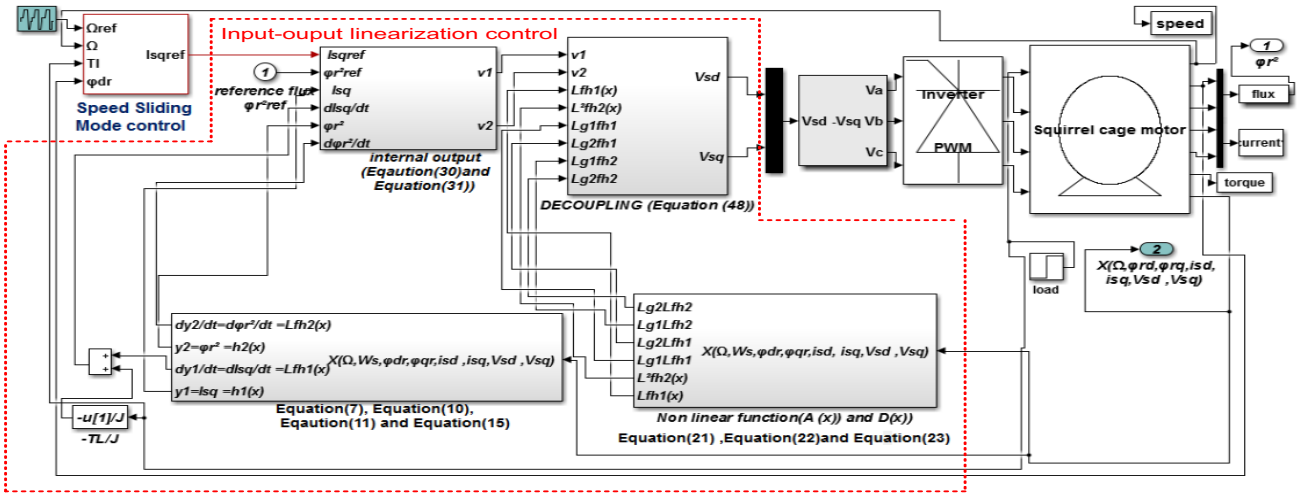

Fig. 1 – Sliding input-output linearization control of squirrel cage motor.

Figure 2 shows the structure of SIOLC, composed of two controls: the speed sliding mode controller, which contains the equivalent control ($I_{sq\text{-}eq}$), calculated using the surface theorem, the surface derivative, and the steady state sliding mode condition. The other is the discontinuous control or correction factor (I_{sqn}), given by the nonlinear saturation function. The output of the speed sliding mode controller is the I_{sqref} current, which is an input to the internal output V_1 of the input-output linearization control.

The central goal of input-output linearization is to design a nonlinear control law, as assumed that the inner loop control is, in the most suitable case, precisely linearized the nonlinear system after appropriate state space modification of coordinates. The developer can then build an outer-loop-control in the new coordinates to obtain a linear relationship between the output Y_1, Y_2 and the internal input V_1, V_2 and to satisfy the traditional control design specifications such as tracking and disturbance rejection.

The internal inputs (V_1, V_2) pass through the linearizing expressions, simultaneously decoupling the control variables. The original system will continue receiving the inputs V_{ds}, V_{qs} which are handled by the linearizing block to comply with the linearity between inputs V_1, V_2 and outputs y_1,y_2.

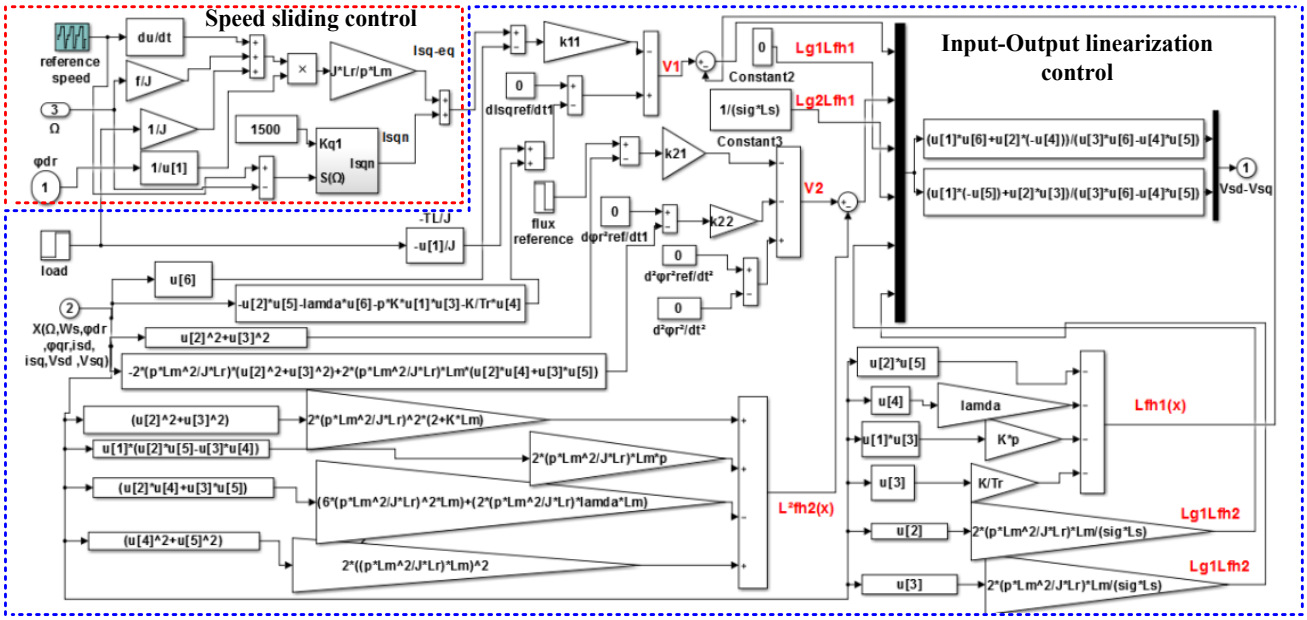

Fig. 2 – Structure of sliding input-output linearization control.

5. SIMULATION RESULTS AND DISCUSSIONS

In Fig. 3, the machine is applied with a load torque of 10 Nm in a time interval [0.26, 0.75] s and [1.91, 2.3] s. The machine's rotation direction is reversed from 157 rad/s to -100 rad/s in time 2.79 s. When the motor is started with the reference speed of 50 rad/s in the time interval [0.05, 1] s, in the input-output linearization control, the speed returns to its reference after overshooting during the transient regime. When the direction of rotation is reversed, the speed overshoots and then follows its reference in the steady state. The load torque application causes a slight decrease in speed, which is quickly rejected.

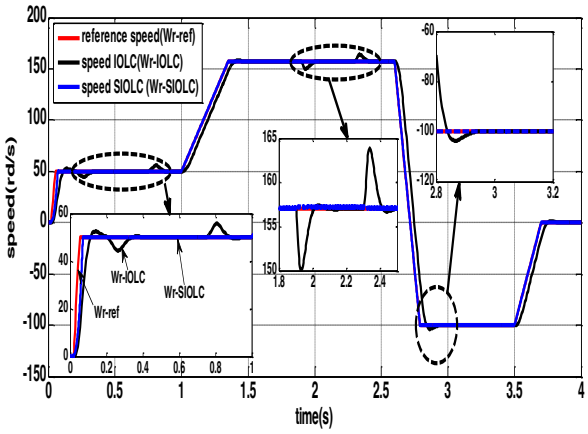

Fig. 3 – Speed result of input-output linearization control (IOLC) and sliding input-output linearization control (SIOLC).

The simulation results show that the sliding input-output linearization control (SIOLC) is robust to the variation of the reference speed since the speed follows the reference speed at start-up as well as the reversal of the direction of rotation, in a very satisfactory way, the application of load torque does not influence the speed response.

In Fig. 4, the sliding input-output linearization control (SIOLC) ensures the robustness of this technique to high and low-speed variations as well as the application of load torque (T_l=10 Nm) in the time interval [0.26, 0.75] s and [0.91, 2.3] s. Concerning the input-output linearization control (IOLC) can lead to a degradation of the expected performances, mainly regarding the tracking of the reference speed and the application of load torque.

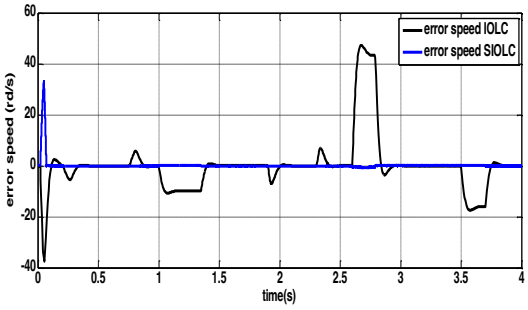

Fig. 4 –Error speed result of Input-output linearization control (IOLC) and sliding input-output linearization control (SIOLC).

From the Figs. 5 and 6, SIOLC performs better and is more capable of forcing flux and torque to track its reference, which means the robustness of SIOLC is stronger than IOLC, which reduces the system's robustness.

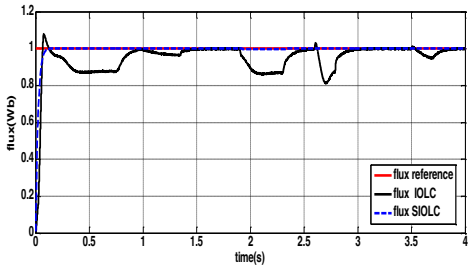

Fig. 5 –Flux result of Input-output linearization control (IOLC) and sliding input-output linearization control (SIOLC).

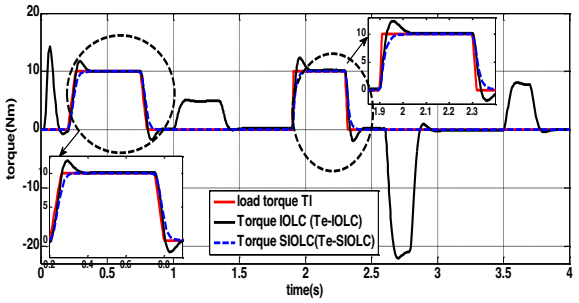

Fig. 6 – Torque result of Input-output linearization control (IOLC) and sliding input-output linearization control (SIOLC).

5.1 ROBUSTNESS TESTS

The results confirm the performances obtained by SIOLC via the variation of the rotor resistance (Rr) in the time interval [1.5, 2] s and inertia moment (J) in the time interval [1.5, 2.4] s. Figs 7 and 8 illustrate the dynamic response of the rotor speed and speed error of SIOLC and IOLC. SIOLC shows that the speed follows its reference with remarkable accuracy against rotor resistance (Rr) variations at high and low speeds compared to IOLC, which shows an oscillation and overshoot on speed and error speed response.

From Figs 9 and 10, SIOLC shows that the torque and flux response is not influenced by the variation of the rotor resistance compared to IOLC, where the torque response contains ripples as well as noticing a minimization of the flux amplitude during the minimization of the rotor resistance value.

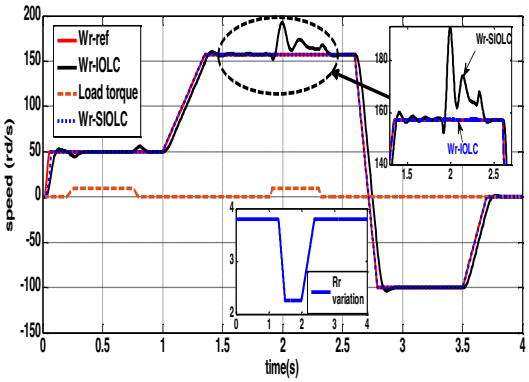

Fig. 7 – Speed result of Input-output linearization control (IOLC) and sliding input-output linearization control (SIOLC) with Rr variation.

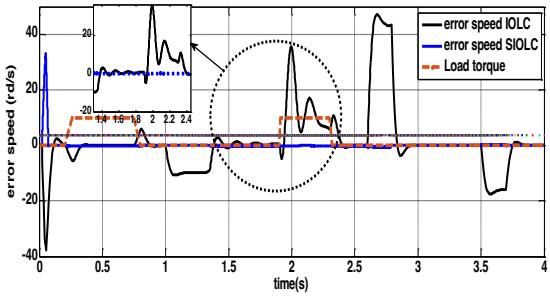

Fig. 8 –Error speed result of Input-output linearization control (IOLC) and sliding input-output linearization control (SIOLC) with R_r variation.

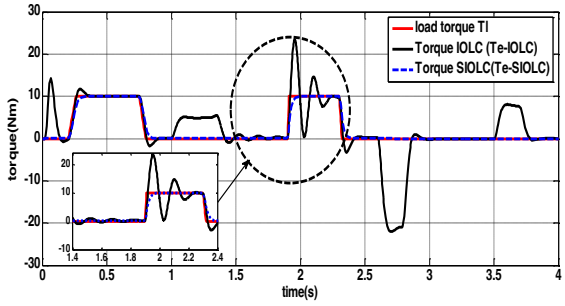

Fig. 9 – Torque result of Input-output linearization control (IOLC) and sliding input-output linearization control (SIOLC) with Rr variation

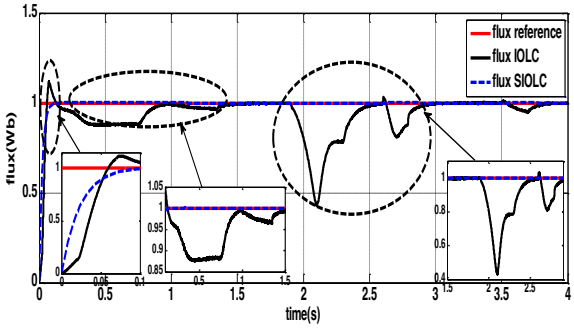

Fig. 10 –Flux result of Input-output linearization control (IOLC) and sliding input-output linearization control (SIOLC) with Rr variation.

From Figs 11 and 12, SIOLC shows that the speed and torque response is not influenced by the variation of the inertia moment (*J*) compared to IOLC where the speed and flux response contains ripples during variation of *J*.

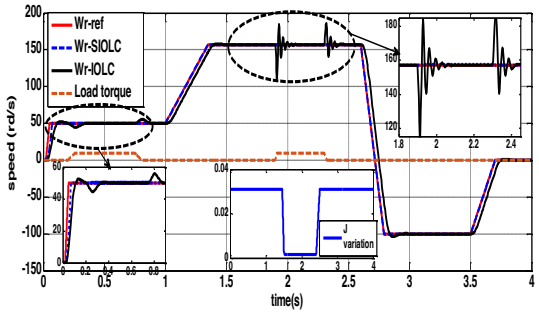

Fig. 11 – Speed result of input-output linearization control (IOLC) and sliding input-output linearization control (SIOLC) with *J* variation.

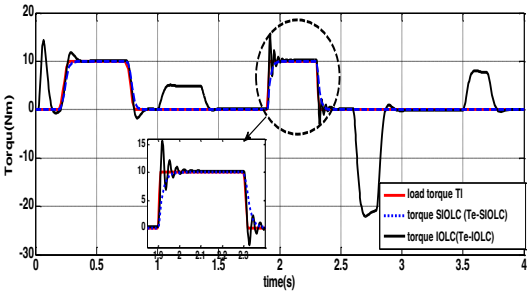

Fig. 12 –Torque result of Input-output linearization control (IOLC) and sliding input-output linearization control (SIOLC) with *J* variation.

7. CONCLUSION

In this paper, we present a study on the combination of two nonlinear controls, the sliding mode control, and the input-

output linearization control, to have a control named the sliding input-output linearization control. The performance analysis of the SIOLC strategy includes the rotor resistance and load torque variations. We validated this method by simulations on a nonlinear model of the squirrel cage motor. The obtained simulation showed that the SIOLC has excellent robustness to parametric uncertainty and disturbances.

Received on 15 December 2022

REFERENCES

1. A. Dendouga, *Feedback linearization associated to a sliding mode controller for an operating with unity power factor of induction motor fed by matrix converter*, SN Applied Sciences. **2**, *5*, pp. 1–7 (2020).
2. Y. Fetene, D. Shibeshi, *Fractional order sliding mode speed control of feedback linearized induction motor,* Power Electronics and Drives. **5**, *41*, pp. 109–122 (2020).
3. S. Zaidi, F. Naceri, R. Abdessemed, *Input-output linearization of in induction motor using MRAS Observer*, International Journal of Advanced Science and Technology. **68**, 2, pp.49–56 (2014).
4. D. Zaghib, A. Allag, M. Allag, B. Hamidani, *Input output linearization control based on a newly extended MVT observer design: an induction machine*, J. of Electrical Engineering. **20**, *5*, pp. 1–7 (2020).
5. O. Oukaci, R. Toufouti, D. Dib, L. Atarsia, *Comparison performance between sliding mode control and nonlinear control application to induction motor*, Electrical Engineering. **99**, *1*, pp. 33–45 (2016).
6. A. Accetta, M. Cirrincione, F. D'ippolito, M. Pucci, A. Sferlazza, Input-output *feedback linearization control of linear induction motor taking into consideration its dynamic end-effects and iron losses*, Conference IEEE Energy Conversion Congress and Exposition (ECCE'2020), Detroit, MI, USA (Oct. 11-15, 2020).
7. A. Alonge, M. Cirrincione, M. Pucci, A. Sferlazza, *Input–output feedback linearization control with online MRAS-based inductor resistance estimation of linear induction motors including the dynamic end effects*, IEEE Transactions on Industry Applications, **52**, *1*, pp 254–266 (2015).
8. F. Berrezzek, W. Bourbia, B. Bensaker, *Nonlinear control of induction motor: a combination of nonlinear observer design and input-output linearization technique*, 4Th International Conference of Electrical Engineering (ICEE'2012), Algeria, (May 08-12, 2012).
9. S. AL-Hashemi1, A. AL-Dujaili1, A.R. Ajel*, Speed control using an integral sliding mode controller for a three-phase induction motor,* Journal of Techniques. **3**, *3*, pp. 10–19 (2021).
10. C. Wang, J. Tang, B. Jiang, Z. Wu, *Sliding-mode variable structure control for complex automatic systems: a survey*, Mathematical Biosciences, and Engineering. **19**, *3*, pp. 2616–2640 (2022).
11. D. Cherifi, Y. Miloud, *Robust speed-sensorless vector control of doubly fed induction motor drive using sliding mode rotor flux observer*, International Journal of Applied Power Engineering, **7**, *3*, pp. 235–250 (2018).
12. K. Venkateswarlu, G. Sandeep, N. Srinivas, K.D. Reddy, *Speed sensorless sliding mode control of induction motor using Simulink*, IOSR Journal of Electrical and Electronics Engineering, **6**, *2*, pp. 50–56 (2013).
13. K.M. Siddiqui, K. Sahay, V.K. Giri, *Modelling and simulation of variable speed squirrel cage induction motor drives*, International Journal of Advanced Research in Electrical, Electronics and Instrumentation Engineering, **4**, *7*, pp. 6720–6728 (2015).
14. A. Mechernene, M. Loucif, M. Zerikat, *induction motor control based on a fuzzy sliding mode approach,* Rev. Roum. Sci. Techn. – Électrotechn. Et Énerg., **64**, *1*, pp. 39–44 (2019).
15. A. Ounissi, A. Kaddouri, M.S. Aggoun, R. Abdessemed, *Second order sliding mode controllers of micropositioning stage piezoelectric actuator Withcolman-Hodgdon model parameters,* Rev. Roum. Sci. Techn. – Électrotechn. Et Énerg., **67**, *1*, pp. 41–46 (2022).